Porous Cellulose Nanofiber (CNF)-based Aerogel with the Loading of Zeolitic Imidazolate Frameworks-8 (ZIF-8) for Cu(II) Removal from Wastewater

Wanyao Meng, Sijie Wang, Haifeng Lv, Zhenxing Wang, Xuewen Han, Zijing Zhou, and Junwen Pu *

A novel biobased porous aerogel was synthesized using physical mixing, freeze-drying, and *in-situ* growth methods. Zeolitic imidazolate frameworks-8 (ZIF-8) were grafted onto the surface of the CS/CNF solid composite to form a ZIF-8@CS/CNF aerogel. The structural characteristics and the adsorption potential of the ZIF-8@CS/CNF aerogel were investigated. It was found that the specific surface area of the ZIF-8@CS/CNF aerogel was 206 m^2/g, and the water stability of the CNF aerogel was enhanced by incorporating the CS. Meanwhile, the adsorption isotherm and kinetics of the composite aerogel fit the pseudo-second-order kinetic model (R^2 = 0.96) and the Langmuir isotherm model (R^2 = 0.97) with the copper(II) oxide (Cu(II)) theoretical adsorption capacity of 245 mg/g, respectively. Furthermore, this aerogel, which combined metal-organic frameworks (MOFs) and CNF, was easy to fabricate and it was biodegradable. These characteristics suggest it has a broad potential for wastewater treatment.

INTRODUCTION

With the vigorous development of industry and agriculture, the discharge of pollutants has posed an enormous challenge to the water environment (Muhamad *et al.* 2018). Heavy metals exist in industrial emissions. They are toxic, harmful, and cause severe damage to the human and natural environment due to their non-biodegradable and bioaccumulation characteristics (Tang *et al.* 2019; Li and Xu 2021). For instance, copper(II) (Cu(II)) oxide is a common natural substance that is widely used in commercial applications, such as in the electrical industry or in antifouling paints. Meanwhile, Cu(II) is also an indispensable trace ion for human beings (Wan *et al.* 2010; Fu and Wang 2011; Fu and Xi 2020). When the body intakes too much copper, it can be noxious to humans, causing liver function damage and cancer (Uauy *et al.* 2008; Anush *et al.* 2020).

Currently, heavy metals are removed from wastewater *via* flotation (Colic *et al.* 2007), chemical precipitation (Chen *et al.* 2018), membrane systems (Liu *et al.* 2019), and adsorption (Zhao *et al.* 2011), among others. Among these methods, adsorption is considered the most promising available technique due to it has high removal rate, simplicity, and wide range of adaptation (Zhou *et al.* 2020). A variety of porous materials

have been used for water treatment because of their high surface area. Some examples include activated carbon (Rao *et al.* 2009), clays (Gu *et al.* 2019), aerogels (Maleki 2016), metal-organic frameworks (MOFs) (Maleki *et al.* 2015), graphene (Liu *et al.* 2020), and polysaccharides (Musarurwa and Tavengwa 2020). However, many adsorbents have limitations, such as a high cost, low adsorption capacity, single synthesis condition, poor controllability, non-biodegradability, and non-renewability. Therefore, a novel, high selectivity adsorbent has been found for the environment and water decontamination. Metal-organic frameworks are a novel high porosity crystal hybrid material. There are numerous advantages with MOFs, such as high specific surface area, easy functionalization, tunable pore structures, simple preparation methods, and chemical stability (Schejn *et al.* 2014; Jian *et al.* 2015; Xiao *et al.* 2019; Xu *et al.* 2021). Therefore, MOFs can be widely used in drug delivery, gas storage and separation, water purification, and catalysis, which has attracted the attention of many researchers. However, MOFs are powdery nanomaterials. They are easily assembled together and not recycled in the water, which cause another problem of water pollution. In order to avoid the secondary pollution, MOF powders should be loaded with other material by electrostatic action, Van der Waals force, or pi-pi conjugate bonding. Gnanaselvan *et al*. (2018) embedded MOF into cellulose acetate, PES, and PVDF respectively. for removing heavy metal ions from wastewater. Ma *et al*. (2019) prepared a lightweight and porous zeolitic imidazolate frameworks-8@cellulose-nanofiber@cellulose foam using a simple in situ green growth method for gas adsorption and heavy metal ions removal.

Cellulose nanofiber (CNF) aerogels display outstanding performance traits, such as a high porosity rate, a low density, and a high specific surface area. In addition, CNF aerogels are biodegradable, bio-compatibly nontoxic, and they possess hydroxyl function groups (Long *et al.* 2018; Esmaeili *et al.* 2021). The abundant hydroxyl functional groups in CNF allow it to easily bind to different adsorbents. These kinds of nanocellulose-based composite material have shown excellent adsorption capacity (Tshikovhi *et al.* 2020). Yu *et al.* (2020) prepared graphene oxide (GO)/carboxymethyl cellulose nanofibril composite fiber as an adsorbent that is economically competitive with an efficient lead uptake (99.0 mg/g). Jin *et al.* (2019) synthesized carboxymethyl cellulose/MOF beads for the adsorption of lead ions (Pb^{2+}) from an aqueous solution with the maximum adsorption capacity of 132 mg/g. Nevertheless, there is only weak hydrogen bonding between cellulose nanofibers, and these can be directly dispersed in water. Therefore, in order to solve this problem, it is a good choice to introduce new groups to add cross-linking agents (Ngah *et al.* 2011; She *et al.* 2018). Tian *et al.* (2017) used natural CNFs cross-linked with acrylic acid (AA) to remove heavy metal ions, and the CNF-based aerogel formed highly porous networks after cross-linking with the AA. Hong *et al.* (2021) synthesized a three-dimensional (3D) porous polyethylenimine (PEI)/CNF aerogel for copper removal. The combination of the CNF and PEI provides excellent wet stability. However, most of the crosslinking agents are toxic and have complex reaction conditions. Therefore, the combination of natural crosslinking agents and CNF can be considered, such as chitosan (CS) (Luo *et al.* 2015), cyclodextrin (Zhang *et al.* 2015), and sodium alginate (Zhao *et al.* 2021). These natural crosslinking agents are inexpensive, biodegradable, non-poisonous, and renewable. Chitosan is an environmentally friendly, inexpensive, and readily available biomolecule material (Ahmed *et al.* 2020; Zhang *et al.* 2021). Chitosan has two reactive functional groups, amine groups at C_2 and hydroxyl groups at C_3 and C_6 (Yang *et al.* 2014). Due to the amine groups, chitosan is a positively charged natural polymer (Xing *et al.* 2019). The amino groups can chelate with certain metal ions and improve the removal rate of the metal ions (Haripriyan

et al. 2022). Also, it can form hydrogen bonds with cellulose nanofibers (Bao *et al.* 2015).

In this paper, zeolitic imidazolate frameworks-8 (ZIF-8) loaded CS/CNF composite was prepared *via* an initial one-pot synthesis. The ZIF-8 crystals were added by *in-situ* growing on the CS/CNF composites to form the ZIF-8@CS/CNF aerogel (Fig. 1). The CNF and CS are sustainable structural materials, with no harmful effects on the environment, human health, or ecosystem. In addition, the CS/CNF composites could help disperse and load the ZIF-8 nanoparticles. The hybrid aerogel exhibited excellent adsorption performances, efficiently collecting heavy metal ions by investigating the adsorption capacity. Therefore, this approach provided a green adsorption material that can efficiently remove Cu(II).
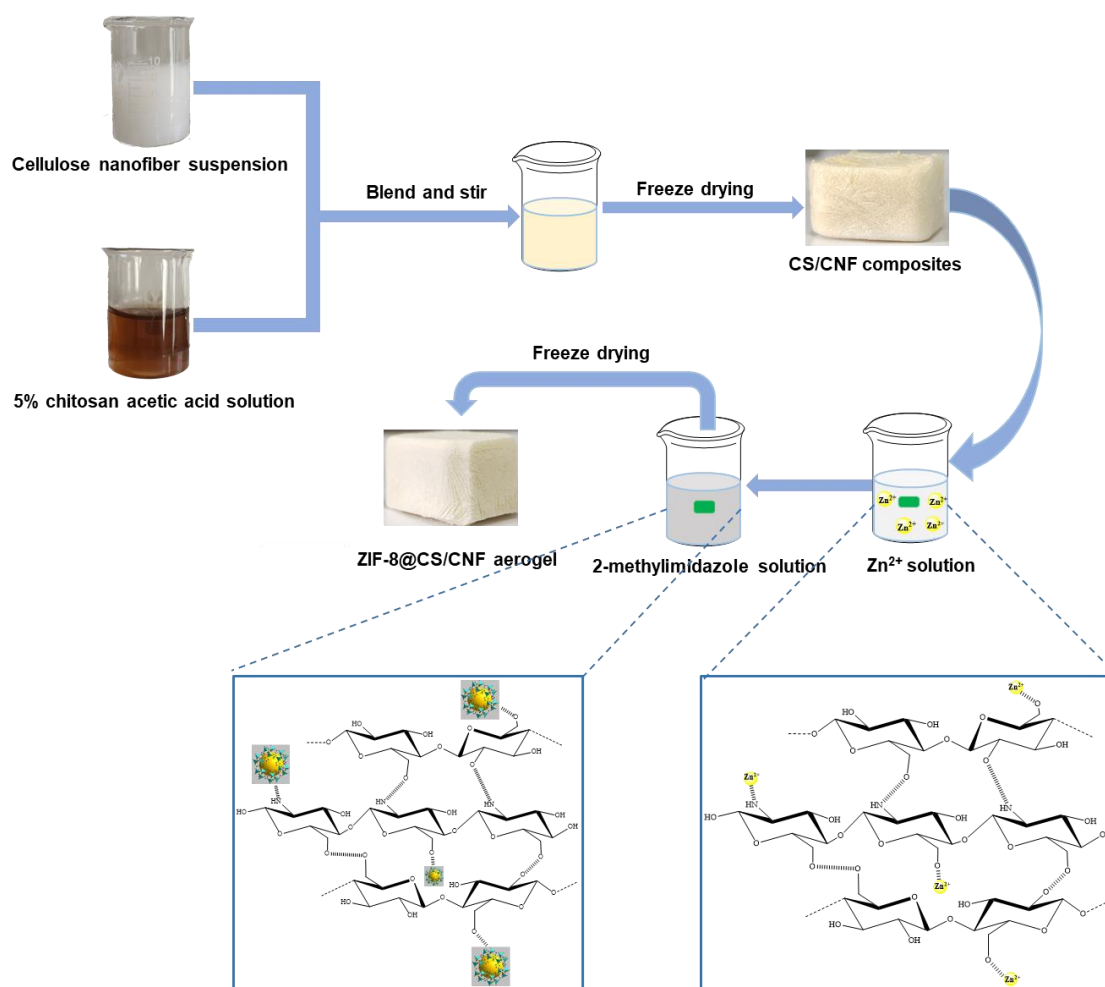

Fig. 1. Schematic illustration of the formation process of the ZIF-8@CS/CNF aerogel

EXPERIMENTAL

Materials

The nanofibrillated cellulose (CNF) suspension of mechanical lapping (1.2% w/v) was obtained from Tianjin Woodelf Biotechnology Co. (Tianjin, China). The chitosan (CS) was supplied by Sinopharm Chemical Reagent Co. (Shanghai, China). The zinc acetate $((CH_3COOH)_2Zn)$ and adsorbate copper chloride $(CuCl_2)$ were purchased from Meryer

Chemical Technology Co. (Shanghai, China). The 2-methylimidazole (2-H-MeIM, $C_4H_6N_2$) was purchased from Shanghai Energy Chemicals Co. (Shanghai, China), and the AA (CH_3COOH) was obtained from Beijing Tongguang Fine Chemical Company (Beijing, China). All the reagents mentioned above were analytically pure without any additional treatment.

Fabrication of the CS/CNF@ZIF-8 Aerogel

Firstly, CS was dissolved in a 2% acetic acid aqueous solution to form a 5% CS solution. Next, 1.25 g of the CS solution (5% w/w) was poured into 5.2 g of CNF suspension (1.2% w/w) and stirred for 30 min to obtain a uniform mixture solution. The CS/CNF compound was acquired by using a vacuum freezer dryer (Free Zone 4.5L; Labconco; USA).

The ZIF-8@CS/CNF aerogel was synthesized in the water by the *in-situ* growth method shown in Fig. 1. Briefly, 2.6 mmol of $(CH_3COOH)_2Zn$ was dissolved to obtain solution A, and 40 mmol 2-methylimidazole was dissolved by deionized water to get solution B. The solid compound of CS/CNF was immersed in solution A for 3 h at room temperature. Next, the CS/CNF composite aerogel was placed into solution A by vacuum pressure processes for 30 min. Subsequently, the Zn^{2+}- CS/CNF composite solid was immersed in solution B in the same way. The ZIF-8@CS/CNF composite aerogel was then prepared by a vacuum freeze dryer. As shown in Fig. 1, -OH and -NH on CS/CNF composites were coordination bonds with Zn^{2+} and 2-methyl imidazole formed with Zn^{2+} by coordination bonds which indicated ZIF-8 was grown on CS/CNF composites (Wang *et al*. 2019).

Characterization

A scanning electron microscope (SEM) (G300; ZEISS, Jena, Germany) was used to examine the surface morphology and structure of the ZIF-8 and the absorbents. Fourier transform infrared spectroscopy (FTIR), ranging 400 to 4000 cm^{-1}, and X-ray diffraction (XRD) were applied to characterize the existence of functional groups and characteristic peaks of the ZIF-8, CNF, and CS. A PerkinElmer Frontier system (Waltham, MA, USA) and a Bruker D8 Advance system (Billerica, MA, USA) were used for the FTIR and XRD analyses, respectively. The specific surfaces of the ZIF-8, CNF/CS aerogel, and ZIF-8@CS/CNF aerogel were measured by the BET method using a specific surface area analyzer (ASAP 2460; Micrometrics, Atlanta, GA, USA).

Adsorption Study

A series of batch adsorption experiments were carried out to study the adsorption capacity of the CS/CNF composite and ZIF-8@CS/CNF aerogel. At a certain temperature, a series of variables were designed, including the different initial Cu^{2+} concentration (400 to 1,000 mg/L), reaction time (0 to 600 min), and pH (2 to 6). For the Cu(II) adsorption measurements, 0.08 g of ZIF-8@CS/CNF aerogel was added to the stoppered glass tubes that contained 20 mL of Cu(II) solution of different concentrations until adsorption equilibrium (600 min). The tubes were then shaken in a thermostatic oscillator (ZWY-2102C; Shanghai Zhicheng Analytical Instrument Manufacturing Co., Ltd; China) at 80 rpm and room temperature.

The concentration of Cu(II) solution before and after adsorption was measured by atomic absorption spectrum (AAS), using a Varian SpectrAA 220 instrument (Victoria, Australia) at a wavelength of 324.7 nm. To evaluate the adsorption capacity of the ZIF-

8@CS/CNF aerogel, the amount of Cu(II) adsorption and the removal efficiency were calculated by Eqs. 1 and 2, respectively (Wang *et al.* 2020),

$$Q_e(mg/g) = \frac{(C_0 - C_e)v}{m} \qquad (1)$$

$$R(\%) = \frac{C_0 - C_e}{C_0} \times 100 \qquad (2)$$

where C_0 is the initial concentration of the Cu(II) solution (mg/L), C_e is the Cu^{2+} concentration of the adsorption equilibrium (mg/L), v is the volume (L) of the Cu^{2+} solution, and m is the quality (g) of the adsorbent.

RESULTS AND DISCUSSION

Characterization

The SEM analysis (Fig. 2) illustrated the morphologies of the CS/CNF composites and ZIF-8@CS/CNF aerogel. As can be seen in Fig. 2, the CS/CNF composites and ZIF-8@CS/CNF aerogel exhibited a 3D porous network structure. It appeared to consist of irregularly shaped interconnected pores with thin walls, which can be attributed to irregular ice crystals that were generated by the freeze-drying technique. The highly porous absorbent would facilitate adsorption capacity because the number of adsorption sites increased. Meanwhile, there were ZIF-8 nanoparticles present in the ZIF-8@CS/CNF aerogel in Fig. 2d. In general, the microscopic morphology exhibited a remarkable difference brought about by the *in-situ* growth of ZIF-8 on the CS/CNF aerogel.
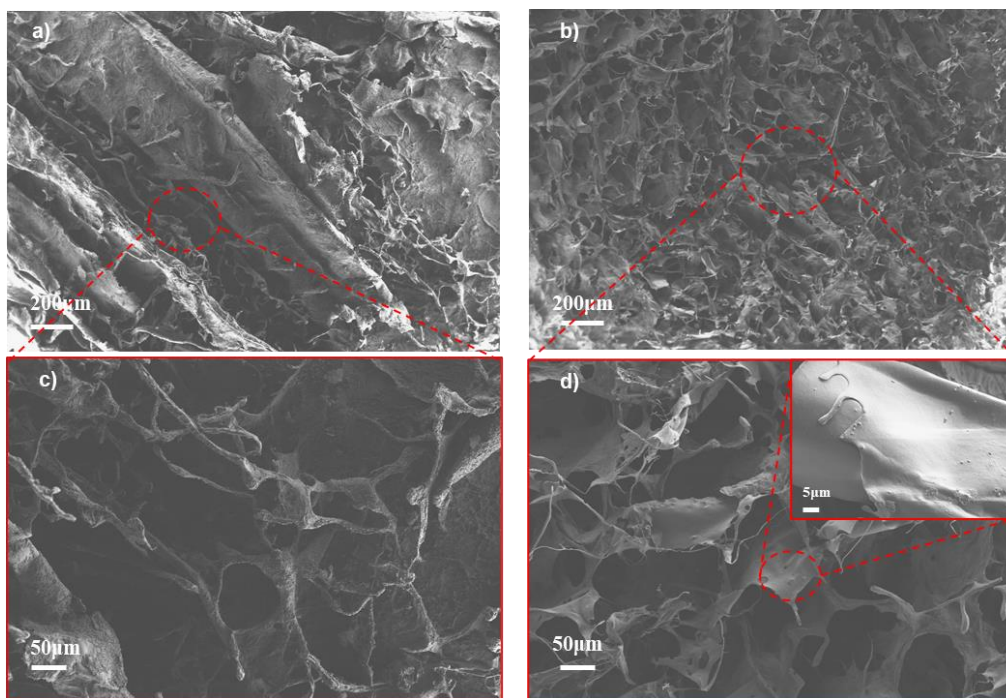

Fig. 2. a) and c) are the SEM images of CS/CNF; b) and d) are the SEM images of the ZIF-8@CS/CNF aerogel; The inset in d) shows the ZIF-8 loaded on the CS/CNF composite aerogel

The N$_2$ isotherm of the adsorbent can well describe the specific surface area of the material, and its data are shown in Table 1. After loading ZIF-8, the specific surface area

of the composites increased significantly. As shown in Fig. 3a, the CS/CNF composite exhibited III type isotherms, indicating that the composite was a macroporous material (Zhao *et al.* 2020). ZIF-8 nanopaticles and ZIF-8@CS/CNF aerogels showed typical I isotherms, indicating that there was mainly microporous adsorption (Sing and Williams 2005). ZIF-8 nanopaticles constitute a highly organic metal skeleton with high porosity (Ren *et al*. 2018). The loading will not destroy the morphology and structure of the composite, and it will increase the specific surface area of ZIF-8@CS/CNF composites aerogels (Thunberg *et al*. 2021). At the same time, the density of the composite aerogels increased with the increase of ZIF-8 loading, while the porosity decreased with the increase of ZIF-8 loading.
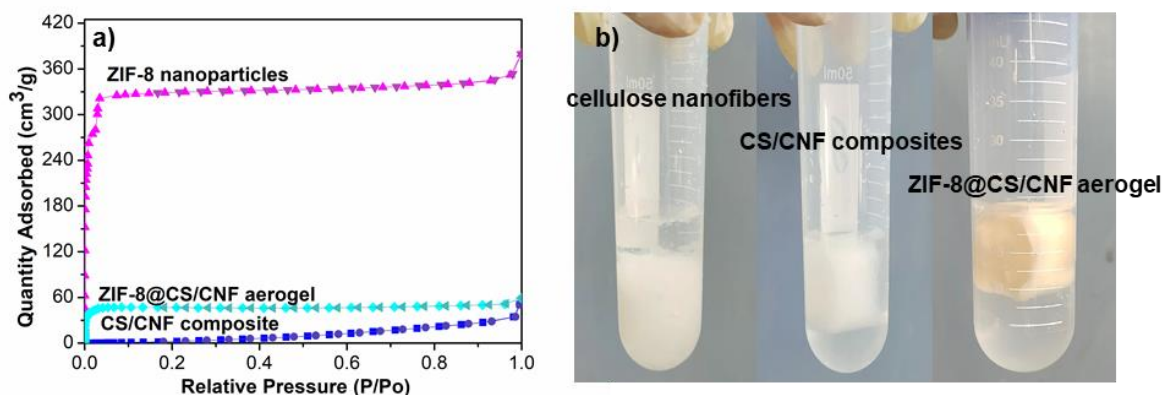

Fig. 3. a) N_2 adsorption-desorption isotherms of ZIF-8 nanoparticles, CS/CNF composites, and ZIF-8@CS/CNF aerogels respectively; b) the water stability of the cellulose nanofibers, CS/CNF composite and ZIF-8@CS/CNF aerogel. The photos illustrate the water stability of the nanofibrillated cellulose, CS/CNF composite and ZIF-8@CS/CNF aerogel.

The stability of aerogels in a water environment was investigated. It can be seen from Fig. 3b that CS/CNF composites and ZIF-8@CS/CNF composites aerogels did not undergo deformation and collapse in water, showing good stability. It might be that CNF can form a good combination with the amino and hydroxyl groups of chitosan through hydroxyl (Xiao *et al*. 2017). In addition, the impregnation solution of the composite aerogels was kept clear, and no turbidity was found between the prepared ZIF-8 materials and the cellulose aerogels. This could be judged to be a stable combination of ZIF-8 and aerogels to a certain extent, and the two strains were not easily separated.

Table 1. Density, Porosity and Specific Surface Area of the Three Materials (ZIF-8 nanoparticles, CS/CNF composite, ZIF-8@CS/CNF aerogel)

Material	Density	Porosity	Specific surface area
ZIF-8 nanoparticles			1621.46 m²/g
CS/CNF composites	0.024 g/cm³	98 %	1.54 m²/g
ZIF-8@CS/CNF aerogel	0.082 g/cm³	91 %	205.81 m²/g

The FTIR spectra of the ZIF-8, the CS/CNF composites, and the ZIF-8@CS/CNF aerogel samples are shown in Figs. 4a and 4b. The FTIR spectrum of the CS/CNF composites exhibited the characteristic peak of CNF and CS at 3347, 2923, 1591, and 1372 cm^{-1}, representing O−H and N−H stretch vibration peaks that overlap to form a broad peak, C−H stretch vibration, −NH$_2$ bending, and CH$_3$ and CH$_2$ stretch vibration, respectively

(Lim and Hudson 2004; Wang *et al.* 2021). After the ZIF-8 was synthesized by *in-situ* on the CS/CNF composites, new stretching bands at 748 and 673 cm^{-1} appeared in the FTIR spectra. These bands represented the typical bands of ZIF-8 molecules, with N−H and out-of-plane bending vibration of imidazole (Bo *et al*. 2018). Meanwhile, the decreased intensity at 2900 to 3500 cm^{-1} demonstrated the interaction between the ZIF-8 and the CNF. The FTIR spectra of the ZIF-8@CS/CNF sample confirmed that the ZIF-8 was successfully grafted onto the CS/CNF composites by the *in-situ* method.
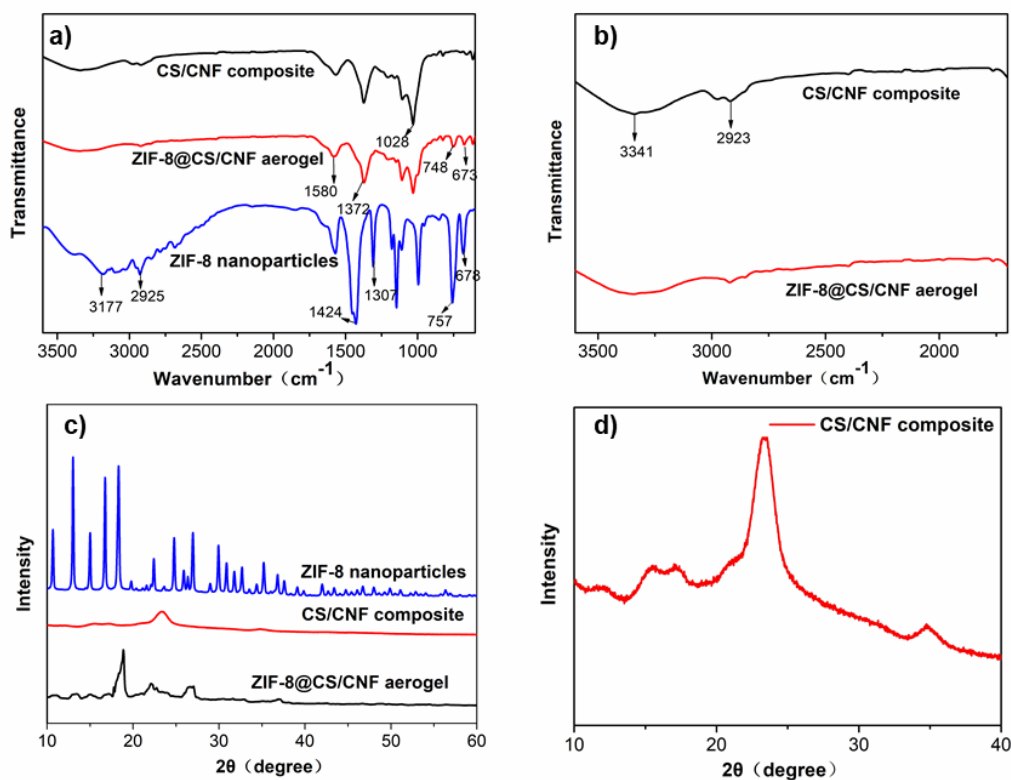

Fig. 4 The a) FTIR spectra of the pure ZIF-8 nanoparticles, the CS/CNF composite, and the ZIF-8@CS/CNF aerogel; the b) enlargement of the FTIR spectra of the CS/CNF composite and the ZIF-8@ CS/CNF aerogel; the c) XRD pattern of the pure ZIF-8 nanoparticles, the CS/CNF composites, and the ZIF-8@ CS/CNF aerogel; the d) enlargement of the XRD pattern of CS/CNF composites

Figure 4c shows the XRD patterns of the synthesized ZIF-8 nanoparticles, the CS/CNF composites, and the ZIF-8@CS/CNF aerogel. The XRD pattern of the CS/CNF composites displayed a sharp peak at $2\theta = 23.4°$ and two weak peaks at $2\theta = 15.4°$ and 34.7°, exhibiting a typical diffraction pattern of cellulose I (Chook *et al*. 2015). Meanwhile, Fig. 4d showed the characteristic peaks at $2\theta = 11.8°$ and 21.3°, which indicated the crystalline nature of CS (Sarkar *et al.* 2017). The XRD spectra of the ZIF-8@CS/CNF aerogel showed the new characteristic peaks at $2\theta = 10.7°$, 13.0°, 14.9°, 16.7°, 18.3°, and 26.9°, which were the characteristic peaks of ZIF-8, in accordance with the reported literature (Venna *et al.* 2010). These results indicated that the ZIF-8 was successfully grown on the CS/CNF aerogel.

Copper Adsorption Experiments

The solution pH of the copper solution is a critical parameter for the adsorption behavior of the adsorbent. The pH value can affect the adsorption site and the physicochemical status of heavy metal ions. For example, Cu(II) was transformed sediment (Cu(OH)$_2$) when the pH was greater than 6.5 (Liu *et al.* 2017). Therefore, a pH range between 2 and 6 was chosen to study its effect on the ZIF-8@CS/CNF aerogel adsorption capacity. The results in Figure 5a showed that the adsorption capacity declined as the pH value decreased from 5 to 2. This might be due to partial amino protonation and structural collapse of ZIF-8 under strong acid condititon (Li *et al*. 2021). Also, there is protonantion of amino of chitosan under acidic solution conditions. When pH = 6, it can be observed that the adsorption capacity is small, which is possible that there may be a small amount of Cu(OH)$_2$ precipitation in the solution (Zhang *et al*. 2016). Therefore, a pH value of 5 was selected as the optimum pH value for further experiments with high uptake performance.
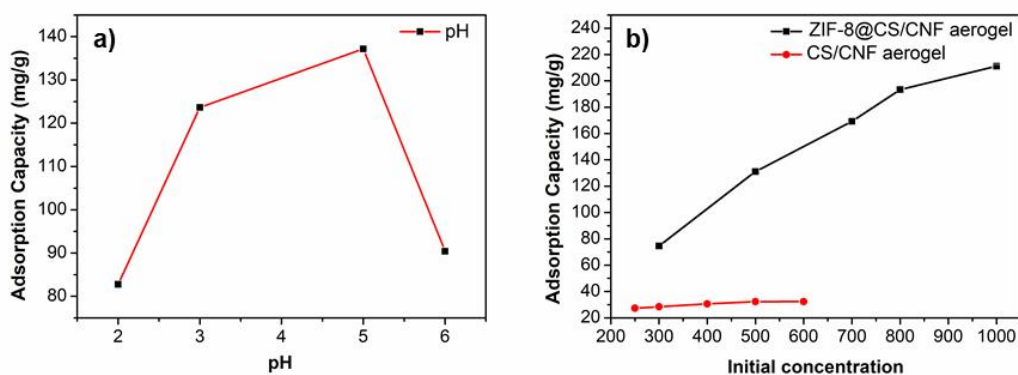

Fig. 5. The a) the effect of the pH on the Cu(II) adsorption with the ZIF-8@CS/CNF aerogel and the b) the adsorption capacity of ZIF-8@CS/CNF and CS/CNF aerogel at different initial concentrations.

Figure 5b shows the adsorption results of ZIF-8@CS/CNF aeogel and CS/CNF composite at different initial concentrations. The results showed that the adsorption capacity of CS/CNF composite doped with ZIF-8 was greatly increased. To help analyze the adsorption of Cu(‖) solution, the Langmuir and Freundlich models fit the experimental adsorption data. Usually, the equations of the Langmuir isotherm (Eq. 3) and the Freundlich isotherm (Eq. 4) are presented as follows (Gupta and Pathak 2021):

$$\frac{C_e}{Q_e} = \frac{1}{Q_{max}}C_e + \frac{1}{k_L Q_{max}} \tag{3}$$

$$lnQ_e = lnk_F + \frac{1}{n}lnC_e \tag{4}$$

where Q_e and Q_{max} are the adsorption capacity at equilibrium (mg/g) and the maximum adsorption capacity of the absorbent (mg/g), respectively, k_L is the adsorption constant of Langmuir isotherm model, k_F is the Freundlich constant, and $1/n$ is the empirical parameter in the Freundlich model, which represents the affinity between the adsorbent and the adsorbate.

Figure 6 shows the plots of Langmuir and Freundlich isothermal models of two composites. The calculated parameters of the two models are summarized in Table 2. As is well-known, the *n* parameter indicates the interaction occurred during the adsorption process. When *n* is greater than 1, it indicates a chemical interaction, when *n* is less than 0,

it denotes the physical interaction, and when *n* is equal to 1, it indicates that no adsorption process that will occur. In this work, *n* greater than 1 represented the chemical interaction in the adsorption process (Chee *et al.* 2021). Also, it can be seen from Table 2 that the correlation coefficients of Langmuir and Freundlich isothermal models were more than 0.95, which can well reveal the adsorption data. This suggests that the adsorption sites were uniformly distributed in the aerogel and may represent a monolayer adsorption (Spagnol *et al.* 2012; Wang *et al.* 2020). According to the Langmuir model, the maximum adsorption capacity of the ZIF-8@CS/CNF aerogel and CS/CNF composite on Cu(II) was 245 mg/g and 36.1 mg/g respectively. In addition, the maximum adsorption capacity was compared to these previously reported adsorbents.
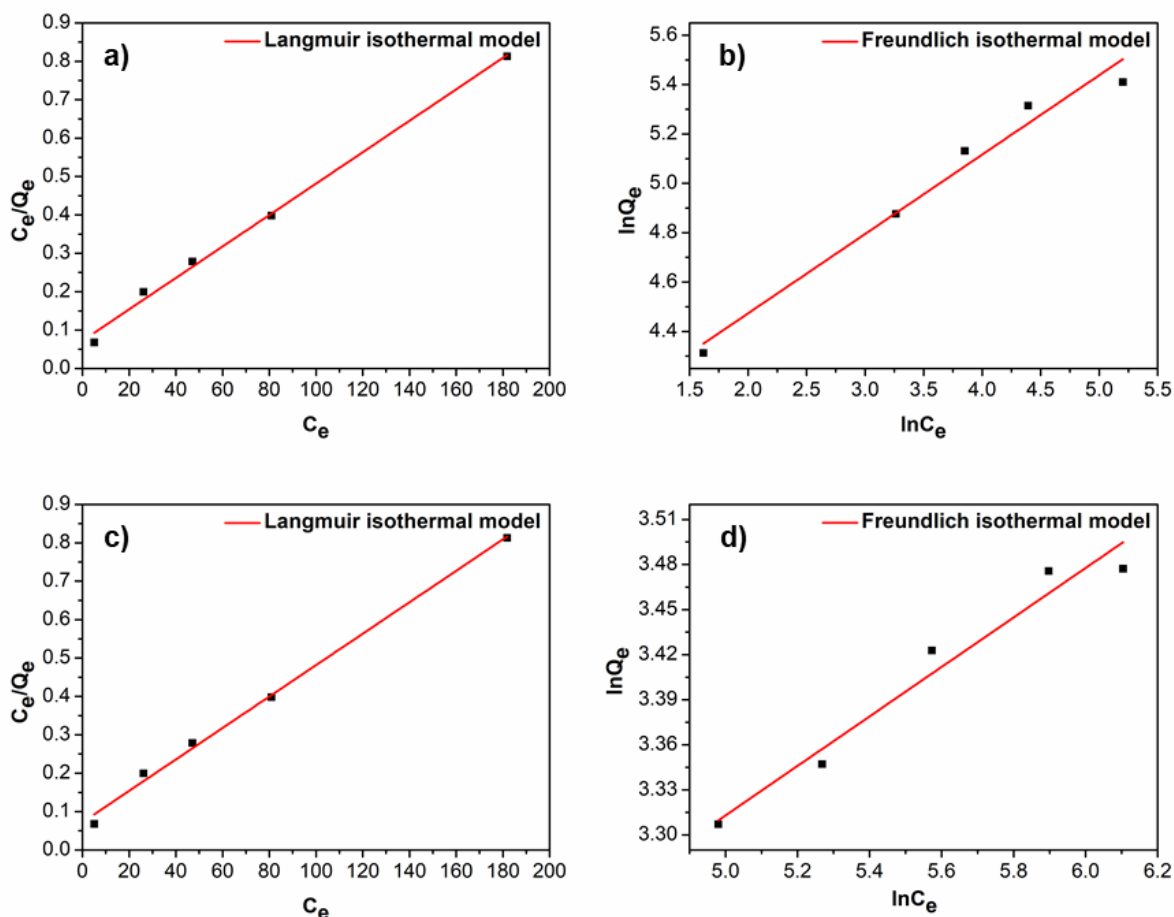

Fig. 6. The a) Langmuir adsorption isotherm plots of the ZIF-8@CS/CNF aerogel; the b) Freundlich adsorption isotherm plots of the ZIF-8@CS/CNF aerogel; the c) and d) is Langmuir adsorption isotherm plots and Freundlich adsorption isotherm plots of the CS/CNF composite, respectively

bioresources.com

Table 2. Langmuir and Freundlich Parameters for the Adsorption Isotherms of the ZIF-8@CS/CNF Aerogel

ZIF-8@CS/CNF Aerogel			CS/CNF Composite		
Isotherm Models	Parameters	Metal Ions (Cu(II))	Isotherm Models	Parameters	Metal Ions (Cu(II))
Langmuir Isotherm	k_L	0.04	Langmuir Isotherm	k_L	0.02
	Q_{max} (mg/g)	244.99		Q_{max}(mg/g)	36.13
	R^2	0.99		R^2	0.99
Freundlich Isotherm	k_F	46.06	Freundlich Isotherm	k_F	12.06
	n	3.11		n	6.07
	R^2	0.97		R^2	0.95
Separation factor	R_L	0.03 to 0.07	Separation factor	R_L	0.08 to 0.17

The data listed in Table 3 demonstrate that the maximum adsorption capacity of the ZIF-8@CS/CNF aerogel for the removal of Cu(II) was higher than recently reported in the literature.

To determine the feasibility and suitability of the ZIF-8@CS/CNF aerogel, the isotherm data separation factor (R_L) was calculated in terms of the Langmuir isotherm data. The separation factor equation can be seen below in Eq. 5,

$$R_L = \frac{1}{1+K_L C_0} \qquad (5)$$

If R_L ranges between 0 and 1, it is beneficial to the adsorption process. If R_L is greater than 1, it is disadvantageous. If R_L is equal to 0, the process is irreversible. The results shown in Table 2 indicated that the ZIF-8@CS/CNF aerogel had a beneficial ability to remove Cu(II).

Table 3. Maximum Capacity of Various Adsorbents for Cu(II) in the Literature

Material	pH	Q_{max} (mg/g)	References
CNF/PVA/AA	6	30.00	(She *et al.* 2018)
CNF/AA	6	40.01	(Tian *et al.* 2017)
CNF/PEI	6	135.10	(Hong *et al.* 2021)
PVA/SA@ZIF-8		166.94	(Zhang *et al.* 2021)
CS/PVA/TEOS beads	6	224.60	(Kamal *et al.* 2014)
CS/CNF	6	36.13	This work
ZIF-8@CS/CNF	5	234.19	This work

The ZIF-8@CS/CNF aerogel was used to learn the adsorption kinetics, and Fig. 7a showed the adsorption behaviors of the aerogel under the initial concentration of 500 mg/L.
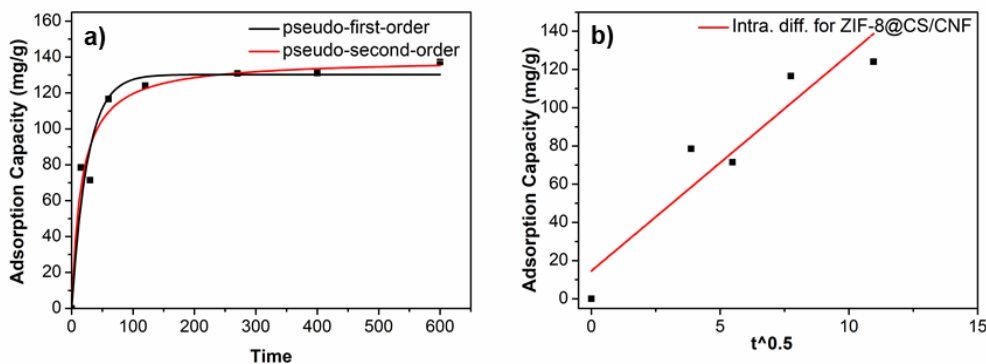
bioresources.com

Fig. 7. The a) pseudo-first-order dynamics and pseudo-second-order dynamics of the ZIF-8@CS/CNF aerogel, the b) intraparticle diffusion of the ZIF-8@CS/CNF aerogel

As can be seen in Fig. 7a, the Cu(Ⅱ) adsorption process exhibited two stages (Qadeer 2013). First, the adsorption capacity increased rapidly during 0 ~ 60 minutes. Secondly, after 300 minutes, the adsorption was close to equilibrium. To explain the adsorption process and efficiency, the experimental results were analyzed based on the pseudo-first-order model (Eq. 6), the pseudo-second-order model (Eq. 7), and the intraparticle diffusion model (Eq. 8) (Shen *et al.* 2020),

$$\ln(Q_e - Q_t) = lnQ_e - k_1 t \tag{6}$$

$$\frac{t}{Q_t} = \frac{1}{(k_2 Q_e^2)} + \frac{t}{Q_e} \tag{7}$$

$$Q_t = K_{id} t^{0.5} + C \tag{8}$$

where Q_t is the adsorption capacity (mg/g) at time t (min), k_1 is the rate constant of the pseudo-first-order adsorption kinetic model, k_2 is the rate constant of the pseudo-second-order adsorption kinetic model, and K_{id} (mg/(g·min$^{0.5}$)) is the intraparticle diffusion model rate constant.

The experimental data were fitted with nonlinear curves, which are shown in Fig. 7a. The fitted parameters can be seen in Table 4. The regression coefficients of pseudo-second-order model and pseudo-second-order model were more than 0.9, and comparison of data indicates that the R^2 of the pseudo-second-order model was better than the pseudo-first-order model. This suggested that the pseudo-second-order equation was consistent with the main kinetic process (Guo *et al.* 2019). According to the existence of -OH, -NH$_2$ and -NH- groups of ZIF-8@CS/CNF aerogels, which could be speculate that the adsorption process has both chemical and physical effects (Wang *et al*. 2019). To further illustrate the uptake process, the intra-particle diffusion model was considered. As can be seen in Fig. 8b and Table 4, R^2 of intraparticle diffusion model (0.86) express well fitted for the data. The fitting curve did not pass through the origin. This result indicated that intraparticle diffusion was not the only control step of adsorption.

***bioresources*.com**

Table 4. Kinetic Modeling Parameters for Adsorption of the ZIF-8@CS/CNF Aerogel

Kinetic Models	Parameters	Metal Ions
		Cu (II)
Pseudo-first-order	$q_{e;exp}$(mg/g)	137.16
	$q_{e;cal}$(mg/g)	130.23
	k_1	0.04
	R^2	0.94
Pseudo-second-order	$q_{e;exp}$(mg/g)	137.16
	$q_{e;cal}$(mg/g)	138.93
	K_2	4.44
	R^2	0.96
Intraparticle Diffusion Model	K	11.33
	R^2	0.86

CONCLUSIONS

1. An aerosol of zeolitic imidazolate framework with nanofibrillated cellulose (ZIF-8@CS/CNF) for removing Cu(II) from its aqueous solution was synthesized successfully by a facile method.

2. The specific surface area of the CS/CNF composites increased after it was grafted with the ZIF-8, which enhanced the adsorption capacity of the composite aerogel.

3. The adsorption isotherm Cu(II) on the ZIF-8@CS/CNF aerogel obeyed the Langmuir model, and the maximum uptake capacity was 234 mg/g.

4. The ZIF-8@CS/CNF aerogel has a great potential to be applied in adsorbing heavy metals and enlarges the scope of the green substrate for immobilizing ZIF-8 nanoparticles.

ACKNOWLEDGEMENTS

Declaration of Interest Statement
The authors declare no competing financial interest.

REFERENCES CITED

Ahmed, K. B. M., Khan, M. M. A., Siddiqui, H., and Jahan, A. (2020). "Chitosan and its oligosaccharides, a promising option for sustainable crop production- A review," *Carbohydrate Polymers* 227, 115331. DOI: 10.1016/j.carbpol.2019.115331

Anush, S. M., Chandan, H. R., Gayathri, B. H., Asma., Manju, N., Vishalakshi, B., and Kalluraya, B. (2020). "Graphene oxide functionalized chitosan-magnetite nanocomposite for removal of Cu(II) and Cr(VI) from waste water," *International Journal of Biological Macromolecules* 164, 4391-4402. DOI: 10.1016/j.ijbiomac.2020.09.059

Bao, W.-Y., Xu, C., Song, F., Wang, X.-L., and Wang, Y.-Z. (2015). "Preparation and properties of cellulose/chitosan transparent films," *Acta Polymerica Sinica* 1, 49-56

Bo, S., Ren, W., Lei, C., Xie, Y., Cai, Y., Wang, S., Gao, J., Ni, Q., and Yao, J. (2018). "Flexible and porous cellulose aerogels/zeolitic imidazolate framework (ZIF-8) hybrids for adsorption removal of Cr(IV) from water," *Journal of Solid State Chemistry* 262, 135-141. DOI: 10.1016/j.jssc.2018.02.022

Chee, D. N. A., Aziz, F., Amin, M. A. M., and Ismail, A. F. (2021). "Copper adsorption on ZIF-8/alumina hollow fiber membrane: A response surface methodology analysis," *Arabian Journal for Science and Engineering* 46(7), 6775-6786. DOI: 10.1007/s13369-021-05636-1

Chen, Q., Yao, Y., Li, X., Lu, J., Zhou, J., and Huang, Z. (2018). "Comparison of heavy metal removals from aqueous solutions by chemical precipitation and characteristics of precipitates," *Journal of Water Process Engineering* 26, 289-300. DOI: 10.1016/j.jwpe.2018.11.003

Chook, S. W., Chia, C. H., Chan, C. H., Chin, S. X., Zakaria, S., Sajab, M. S., and Huang, N. M. (2015). "A porous aerogel nanocomposite of silver nanoparticles-functionalized cellulose nanofibrils for SERS detection and catalytic degradation of rhodamine B," *RSC Advances* 5(108), 88915-88920. DOI: 10.1039/c5ra18806g

Colic, M., Morse, W., and Miller, J. D. (2007). "The development and application of centrifugal flotation systems in wastewater treatment," *International Journal of Environment and Pollution* 30(2), 296-312. DOI: 10.1504/IJEP.2007.014706

Esmaeili, Z., Izadyar, S., Hamzeh, Y., and Abdulkhani, A. (2021). "Preparation and characterization of highly porous cellulose nanofibrils/chitosan aerogel for acid blue 93 adsorption: Kinetics, isotherms, and thermodynamics analysis," *Journal of Chemical & Engineering Data* 66(2), 1068-1080. DOI: 10.1021/acs.jced.0c00872

Fu, F., and Wang, Q. (2011). "Removal of heavy metal ions from wastewaters: A review," *Journal of Environmental Management* 92(3), 407-418. DOI: 10.1016/j.jenvman.2010.11.011

Fu, Z., and Xi, S. (2020). "The effects of heavy metals on human metabolism," *Toxicology Mechanisms and Methods* 30(3), 167-176. DOI: 10.1080/15376516.2019.1701594

Gnanasekaran, G., Balaguru, S., Arthanareeswaran, G., and Das, D. B. (2019). "Removal of hazardous material from wastewater by using metal organic framework (MOF) embedded polymeric membranes," *Separation Science and Technology* 54(3) 434-446. DOI: 10.1080/01496395.2018.1508232

Gu, S., Kang, X., Wang, L., Lichtfouse, E., and Wang, C. (2019). "Clay mineral adsorbents for heavy metal removal from wastewater: A review," *Environmental Chemistry Letters* 17(2), 629-654. DOI: 10.1007/s10311-018-0813-9

Guo, X., and Wang, J.-L., (2019). "A general kinetic model for adsorption: Theoretical analysis and modeling," *Journal of Molecular Liquids* 288, 111100. DOI: 10.1016/j.molliq.2019.111100

Gupta, R., and Pathak, D. D. (2021). "Surface functionalization of mesoporous silica with maltodextrin for efficient adsorption of selective heavy metal ions from aqueous solution," *Colloids and Surfaces A: Physicochemical and Engineering Aspects* 631, 127695. DOI: 10.1016/j.colsurfa.2021.127695

Haripriyan, U., Gopinath, K.-P., and Arun, J. (2022). "Chitosan based nano adsorbents and its types for heavy metal removal: A mini review," *Materials Letters* 312. DOI: 10.1016/j.matlet.2022.131670

Hong, H.-J., Ban, G., Kim, H. S., Jeong, H. S., and Park, M. S. (2021). "Fabrication of cylindrical 3D cellulose nanofibril (CNF) aerogel for continuous removal of copper(Cu^{2+}) from wastewater," *Chemosphere* 278, 130288. DOI: 10.1016/j.chemosphere.2021.130288

Jian, M., Liu, B., Liu, R., Qu, J., Wang, H., and Zhang, X. (2015). "Water-based synthesis of zeolitic imidazolate framework-8 with high morphology level at room temperature," *RSC Advances* 5(60), 48433-48441. DOI: 10.1039/c5ra04033g

Jin, H.-X., Xu, H. P., Wang, N., Yang, L.-Y., Wang, Y.-G., Yu, D., and Ouyang, X.-K. (2019). "Fabrication of carboxymethylcellulose/metal-organic framework beads for removal of Pb(II) from aqueous solution," *Materials* 12(6). DOI: 10.3390/ma12060942

Kamal, M. A., Yasin, T., Reinert, L., and Duclaux, L. (2014). "Adsorptive removal of copper (II) ions from aqueous solution by silane cross-linked chitosan/PVA/TEOS beads: Kinetics and isotherms," *Desalination and Water Treatment* 57(9), 4037-4048. DOI: 10.1080/19443994.2014.991761

Li, D., and Xu, F. (2021). "Removal of Cu (II) from aqueous solutions using ZIF-8@GO composites," *Journal of Solid State Chemistry* 302, 122406. DOI: 10.1016/j.jssc.2021.122406

Li, K., Miwornunyuie, N., Chen, L., Huang, J.-Y., Amaniampong, P.-S., Koomson, D.-A., Ewusi-Mensah, D., Xue, W.-C., Li, G.,Lu, H. (2021). "Sustainable application of ZIF-8 for heavy-metal removal in aqueous solutions," *Sustainability* 13(2). DOI: 10.3390/su13020984

Lim, S.-H., and Hudson, S. M. (2004). "Synthesis and antimicrobial activity of a water-soluble chitosan derivative with a fiber-reactive group," *Carbohydrate Research* 339(2), 313-319. DOI: 10.1016/j.carres.2003.10.024

Liu, J., Chen, F., Yao, Q., Sun, Y., Huang, W., Wang, R., Yang, B., Li, W., and Tian, J. (2020). "Application and prospect of graphene and its composites in wastewater treatment," *Polish Journal of Environmental Studies* 29(6), 3965-3974. DOI: 10.15244/pjoes/117660

Liu, J., Su, D., Yao J., Huang Y., Shao Z., and Chen, X. (2017). "Soy protein-based polyethylenimine hydrogel and its high selectivity for copper ions removal in wastewater treatment," *Journal of Materials Chemistry A* 5(8), 4163-4171. DOI: 10.1039/c6ta10814h

Liu, L., Xu, Y., Wang, K., Li, K., Xu, L., Wang, J., and Wang, J. (2019). "Fabrication of a novel conductive ultrafiltration membrane and its application for electrochemical removal of hexavalent chromium," *Journal of Membrane Science* 584, 191-201. DOI: 10.1016/j.memsci.2019.05.018

Long, L.-Y., Weng, Y.-X., and Wang, Y.-Z. (2018). "Cellulose aerogels: Synthesis, applications, and prospects," *Polymers* 10(6), 623. DOI: 10.3390/polym10060623

Luo, X., Zeng, J., Liu, S., and Zhang, L. (2015). "An effective and recyclable adsorbent for the removal of heavy metal ions from aqueous system: Magnetic chitosan/cellulose microspheres," *Bioresource Technology* 194, 403-406. DOI: 10.1016/j.biortech.2015.07.044

Ma, S.-S., Zhang, M.-Y., Nie, J.-Y., Tan, J.-J., Song, S.-X., and Luo, Y.-W. (2019). "Lightweight and porous cellulose-based foams with high loadings of zeolitic imidazolate frameworks-8 for adsorption applications," *Carbohydrate Polymers* 208, 328-335. DOI: 10.1016/j.carbpol.2018.12.081

Maleki, A., Hayati, B., Naghizadeh, M., and Joo, S. W. (2015). "Adsorption of

hexavalent chromium by metal organic frameworks from aqueous solution," *Journal of Industrial and Engineering Chemistry* 28, 211-216. DOI: 10.1016/j.jiec.2015.02.016

Maleki, H. (2016). "Recent advances in aerogels for environmental remediation applications: A review," *Chemical Engineering Journal* 300, 98-118. DOI: 10.1016/j.cej.2016.04.098

Muhamad, N., Abdullah, N., Rahman, M. A., Abas, K. H., Aziz, A. A., Othman, M. H. D., Jaafar, J., and Ismail, A. F. (2018). "Removal of nickel from aqueous solution using supported zeolite-Y hollow fiber membranes," *Environmental Science and Pollution Research* 25(19), 19054-19064. DOI: 10.1007/s11356-018-2074-3

Musarurwa, H., and Tavengwa, N. T. (2020). "Application of carboxymethyl polysaccharides as bio-sorbents for the sequestration of heavy metals in aquatic environments," *Carbohydrate Polymers* 237, article no. 116142. DOI: 10.1016/j.carbpol.2020.116142

Ngah, W. S. W., Teong, L. C., and Hanafiah, M. A. K. M. (2011). "Adsorption of dyes and heavy metal ions by chitosan composites: A review," *Carbohydrate Polymers* 83(4), 1446-1456. DOI: 10.1016/j.carbpol.2010.11.004

Qadeer, R. (2013). "Concentration effects associated with the kinetics of ruthenium ions adsorption on activated charcoal," *Journal of Radioanalytical and Nuclear Chemistry* 295(3), 1649-1653. DOI10.1007/s10967-012-1961-1

Rao, M. M., Ramana, D. K., Seshaiah, K., Wang, M. C., and Chien, S. W. C. (2009). "Removal of some metal ions by activated carbon prepared from *Phaseolus aureus* hulls," *Journal of Hazardous Materials* 166(2-3), 1006-1013. DOI: 10.1016/j.jhazmat.2008.12.002

Ren, W.-J., Gao, J.-K., Lei, C., Xie, Y.-B., Cai, Y.-R., Ni, Q.-Q., and Yao, J.-M. (2018). "Recyclable metal-organic framework/cellulose aerogels for activating peroxymonosulfate to degrade organic pollutants," *Chemical Engineering Journal* 349, 766-774. DOI: 10.1016/j.cej.2018.05.143

Sarkar, G., Orasugh, J. T., Saha, N. R., Roy, I., Bhattacharyya, A., Chattopadhyay, A. K., Rana, D., and Chattopadhyay, D. (2017). "Cellulose nanofibrils/chitosan based transdermal drug delivery vehicle for controlled release of ketorolac tromethamine," *New Journal of Chemistry* 41(24), 15312-15319. DOI: 10.1039/c7nj02539d

Schejn, A., Balan, L., Falk, V., Aranda, L., Medjahdi, G., and Schneider, R. (2014). "Controlling ZIF-8 nano- and microcrystal formation and reactivity through zinc salt variations," *CrystEngComm* 16(21), 4493-4500. DOI: 10.1039/c3ce42485e

She, J., Tian, C., Wu, Y., Li, X., Luo, S., Qing, Y., and Jiang, Z. (2018). "Cellulose nanofibrils aerogel cross-linked by poly(vinyl alcohol) and acrylic acid for efficient and recycled adsorption with heavy metal ions," *Journal of Nanoscience and Nanotechnology* 18(6), 4167-4175. DOI: 10.1166/jnn.2018.15264

Shen, B., Wang, B., Zhu, L., and Jiang, L. (2020). "Properties of cobalt- and nickel-doped Zif-8 framework materials and their application in heavy-metal removal from wastewater," *Nanomaterials* 10(9), 1636. DOI: 10.3390/nano10091636

Sing, K.-S.-W., and Williams, R.-T., (2005). "Empirical procedures for the analysis of physisorption isotherms," *Adsorption Science & Technology* 23(10), 839-853. DOI: 10.1260/026361705777641990

Spagnol, C., Rodrigues, F. H. A., Pereira, A. G. B., Fajardo, A. R., Rubira, A. F., and Muniz, E. C. (2012). "Superabsorbent hydrogel composite made of cellulose nanofibrils and chitosan-*graft*-poly(acrylic acid)," *Carbohydrate Polymers* 87(3),

2038-2045. DOI: 10.1016/j.carbpol.2011.10.017

Tang, J., Song, Y., Zhao, F., Spinney, S., Bernardes, J. S., and Tam, K. C. (2019). "Compressible cellulose nanofibril (CNF) based aerogels produced via a bio-inspired strategy for heavy metal ion and dye removal," *Carbohydrate Polymers* 208, 404-412. DOI: 10.1016/j.carbpol.2018.12.079

Thunberg, J., Zacharias, SC., Hasani, M., Oyetunji, O.-A., Noa, F.-M.-A., Westman, G., Ohrstrom, L. (2021). "Hybrid metal-organic framework-cellulose materials retaining high porosity: ZIF-8@cellulose nanofibrils," *Inorganics* 9(11). DOI: 10.3390/inorganics9110084

Tian, C., She, J., Wu, Y., Luo, S., Wu, Q., and Qing, Y. (2017). "Reusable and cross-linked cellulose nanofibrils aerogel for the removal of heavy metal ions," *Polymer Composites* 39(12), 4442-4451. DOI: 10.1002/pc.24536

Tshikovhi, A., Mishra, S. B., and Mishra, A. K. (2020). "Nanocellulose-based composites for the removal of contaminants from wastewater," *International Journal of Biological Macromolecules* 152, 616-632. DOI: 10.1016/j.ijbiomac.2020.02.221

Uauy, R., Maass, A., and Araya, M. (2008). "Estimating risk from copper excess in human populations," *The American Journal of Clinical Nutrition* 88(3), 867S-871S. DOI: 10.1093/ajcn/88.3.867S

Venna, S. R., Jasinski, J. B., and Carreon, M. A. (2010). "Structural evolution of zeolitic imidazolate framework-8," *Journal of the American Chemical Society* 132(51), 18030-18033. DOI: 10.1021/ja109268m

Wan, M.-W., Kan, C.-C., Rogel, B. D., and Dalida, M. L. P. (2010). "Adsorption of copper (II) and lead (II) ions from aqueous solution on chitosan-coated sand," *Carbohydrate Polymers* 80(3), 891-899. DOI: 10.1016/j.carbpol.2009.12.048

Wang, C., Yang, R., and Wang, H. (2020). "Synthesis of ZIF-8/fly ash composite for adsorption of Cu^{2+}, Zn^{2+} and Ni^{2+} from aqueous solutions," *Materials* 13(1), 214. DOI: 10.3390/ma13010214

Wang, J.-L. and Guo, X. (2020). "Adsorption isotherm models: Classification, physical meaning, application and solving method," *Chemosphere* 258. DOI: 10.1016/j.chemosphere.2020.127279

Wang, S., Meng, W., Lv, H., Wang, Z., and Pu, J. (2021). "Thermal insulating, light-weight and conductive cellulose/aramid nanofibers composite aerogel for pressure sensing," *Carbohydrate Polymers* 270, article no. 118414. DOI: 10.1016/j.carbpol.2021.118414

Wang, Y.-T., Dai, X., Zhan, Y.-X., Ding, X.-Q., Wang, M., and Wang, X.-L. (2019). "In situ growth of ZIF-8 nanoparticles on chitosan to form the hybrid nanocomposites for high-efficiency removal of Congo Red," *International Journal of Biological Macromolecules* 137, 77-86. DOI: 10.1016/j.ijbiomac.2019.06.195

Xiao, M., and Hu, J.-C. (2017). "Cellulose/chitosan composites prepared in ethylene diamine/potassium thiocyanate for adsorption of heavy metal ions," *Cellulose* 24(6), 2545-2557. DOI: 10.1007/s10570-017-1287-9

Xiao, Y., Hong, A. N., Hu, D., Wang, Y., Bu, X., and Feng, P. (2019). "Solvent-free synthesis of zeolitic imidazolate frameworks and the catalytic properties of their carbon materials," *Chemistry–A European Journal* 25(71), 16358-16365. DOI: 10.1002/chem.201903888

Xing, L., Fan, Y.-T., Shen, L.-J., Yang, C.-X., Liu, X.-Y., Ma, Y.-N., Qi, L.-Y., Cho, K.-H., Cho, C.-S., and Jiang, H.-L. (2019). "pH-sensitive and specific ligand-conjugated chitosan nanogels for efficient drug delivery," *International Journal of Biological*

and Macromolecules 141, 85-97. DOI: 10.1016/j.ijbiomac.2019.08237

Xu, G.-R., An, Z.-H., Xu, K., Liu, Q., Das, R., and Zhao, H.-L. (2021). "Metal organic framework (MOF)-based micro/nanoscaled materials for heavy metal ions removal: The cutting-edge study on designs, synthesis, and applications," *Coordination Chemistry Reviews* 427, 213554. DOI: 10.1016/j.ccr.2020.213554

Yang, Y., Wu, W.-q., Zhou, H.-h., Huang, Z.-y., Ye, T.-t., Liu, R., and Kuang, Y.-f. (2014). "Adsorption behavior of cross-linked chitosan modified by graphene oxide for Cu(II) removal," *Journal of Central South University* 21(7), 2826-2831. DOI: 10.1007/s11771-014-2246-3

Yu, H., Hong, H.-J., Kim, S. M., Ko, H. C., and Jeong, H. S. (2020). "Mechanically enhanced graphene oxide/carboxymethyl cellulose nanofibril composite fiber as a scalable adsorbent for heavy metal removal," *Carbohydrate Polymers* 240, 116348. DOI: 10.1016/j.carbpol.2020.116348

Zhao, G., Li, J., Ren, X., Chen, C., and Wang, X. (2011). "Few-layered graphene oxide nanosheets as superior sorbents for heavy metal ion pollution management," *Environmental Science & Technology* 45(24), 10454-10462. DOI: 10.1021/es203439v

Zhao, H., Ouyang, X.-K., and Yang, L.-Y. (2021). "Adsorption of lead ions from aqueous solutions by porous cellulose nanofiber–sodium alginate hydrogel beads," *Journal of Molecular Liquids* 324, 115122. DOI: 10.1016/j.molliq.2020.115122

Zhao, H.-K., Zhang, K.-H., Rui, S.-P., Zhao, P.-P. (2020). "Study on microcrystalline cellulose/chitosan blend foam gel material," *Sci and Engineering of Composite Materials* 27(1), 424-432. DOI: 10.1515/secm-2020-0047

Zhang, F., Wu, W., Sharma, S., Tong, G., and Deng, Y. (2015). "Synthesis of cyclodextrin-functionalized cellulose nanofibril aerogel as a highly effective adsorbent for phenol pollutant removal," *BioResources* 10(4), 7555-7568. DOI: 10.15376/biores.10.4.7555-7568

Zhang, Y.-J., Xie, Z.-Q., Wang, Z.-Q., Feng, X.-H., Wang, Y., and Wu, A.-G. (2016). "Unveiling the adsorption mechanism of zeolitic imidazolate framework-8 with high efficiency for removal of copper ions from aqueous solutions," *Dalton Transactions* 45(32), 12653-12660. DOI: 10.1039/c6dt01827k

Zhang, M., Jiang, S., Han, F., Li, M., Wang, N., and Liu, L. (2021). "Anisotropic cellulose nanofiber/chitosan aerogel with thermal management and oil absorption properties," *Carbohydrate Polymers* 264, 118033. DOI: 10.1016/j.carbpol.2021.118033

Zhang, X., Li, Z.-y., Zhang, T.-y., Chen, Jing., Ji, W.-x., and Wei, Y. (2021). "Fabrication of an efficient ZIF-8 alginate composite hydrogel material and its application to enhanced copper(II) adsorption from aqueous solutions," *New Journal of Chemistry* 45, 15876-15886. DOI: 10.1039/D1NJ03427H

Zhou, L., Li, N., Jin, X., Owens, G., and Chen, Z. (2020). "A new *n*Fe@ZIF-8 for the removal of Pb(II) from wastewater by selective adsorption and reduction," *Journal of Colloid and Interface Science* 565, 167-176. DOI: 10.1016/j.jcis.2020.01.014